Journal of Thrombosis and Haemostasis, **4**: 519–526

IN FOCUS

Increased metastatic potential of tumor cells in von Willebrand factor-deficient mice

V. TERRAUBE,* R. PENDU,† D. BARUCH,* M. F. B. G. GEBBINK,† D. MEYER,* P. J. LENTING,† and C. V. DENIS*

**INSERM U143, Le Kremlin-Bicêtre, France; and †Department of Haematology, The Laboratory for Thrombosis and Haemostasis, University Medical Center Utrecht, Utrecht, The Netherlands*

To cite this article: Terraube V, Pendu R, Baruch D, Gebbink MFBG, Meyer D, Lenting PJ, Denis CV. Increased metastatic potential of tumor cells in von Willebrand factor-deficient mice. *J Thromb Haemost* 2006; **4**: 519–26.

See also Shavit JA, Motto DG. Coagulation and metastasis – an unexpected role for von Willebrand factor. This issue, pp 517–8.

Summary. *Background:* The key role played by von Willebrand factor (VWF) in platelet adhesion suggests a potential implication in various pathologies, where this process is involved. In cancer metastasis development, tumor cells interact with platelets and the vessel wall to extravasate from the circulation. As a potential mediator of platelet–tumor cell interactions, VWF could influence this early step of tumor spread and therefore play a role in cancer metastasis. *Objectives:* To investigate whether VWF is involved in metastasis development. *Methods:* In a first step, we characterized the interaction between murine melanoma cells B16-BL6 and VWF *in vitro*. In a second step, an experimental metastasis model was used to compare the formation of pulmonary metastatic foci in C57BL/6 wild-type and VWF-null mice following the injection of B16-BL6 cells or Lewis lung carcinoma cells. *Results: In vitro* adhesion assays revealed that VWF is able to promote a dose-dependent adhesion of B16-BL6 cells *via* its Arg-Gly-Asp (RGD) sequence. In the experimental metastasis model, we found a significant increase in the number of pulmonary metastatic foci in VWF-null mice compared with the wild-type mice, a phenotype that could be corrected by restoring VWF plasma levels. We also showed that increased survival of the tumor cells in the lungs during the first 24 h in the absence of VWF was the cause of this increased metastasis. *Conclusion:* These findings suggest that VWF plays a protective role against tumor cell dissemination *in vivo*. Underlying mechanisms remain to be investigated.

Keywords: experimental metastasis, melanoma cells, von Willebrand factor-deficient mice.

Correspondence: Cécile V. Denis, INSERM U143, 80 rue du Général Leclerc, 94276 Le Kremlin-Bicêtre cedex, France.
Tel.: +33149595605; fax: +33149595656; e-mail: denis@kb.inserm.fr

Received 15 April 2005, accepted 1 November 2005

Introduction

A tight relationship between the hemostatic system and malignant disease has been recognized for years [1]. An hypercoagulable state is often observed in cancer patients, linked to the capacity of tumor cells to produce directly or indirectly activators of the coagulation cascade as well as activators and inhibitors of the fibrinolytic pathway [2]. Therefore, these patients show an increased susceptibility to develop thromboembolic diseases among which deep vein thrombosis, pulmonary embolism, or disseminated intravascular coagulation are the most common [3]. Another mechanism by which the hemostatic system is linked to cancer development comes from its ability to regulate angiogenesis by a number of proteins secreted by the platelet alpha granules or by cryptic fragments of the coagulation cascade [4].

Among the different players present at the interface between hemostasis and cancer, blood platelets are of particular importance: in 1968, Gasic *et al*. [5] showed that a reduction in platelet number leads to reduced metastasis formation in mice. Metastasis spreading is a multi-step process in which tumor cells separate from a primary tumor, migrate across blood vessel walls into the bloodstream and disperse throughout the body to generate new colonies. Since the work of Gasic, there has been growing evidence that successful metastasis may depend on the ability of tumor cells to interact with platelets [6]. The presence of platelets around them could protect the tumor cells from clearance by the immune system [7]. Alternatively, platelets may mediate tumor cell arrest and adhesion to the endothelium, thus facilitating cell extravasation [8,9]. Among the molecular mechanisms underlying these platelet–tumor cell interactions, some authors have reported the implication of platelet P-selectin [10]. Another pathway may rely on the presence at the tumor cell surface of adhesion receptors normally found on platelets: integrins $\alpha_{IIb}\beta_3$ and $\alpha_v\beta_3$ [9,11] or a glycoprotein Ib-like receptor [12]. The binding of tumor cells to platelets would therefore be reminiscent of platelet aggregation and be mediated by adhesive proteins

[13,14]. In that prospect, one of the most attractive candidates is von Willebrand factor (VWF) whose normal function in primary hemostasis is to promote platelet adhesion to the subendothelium and platelet aggregation. The multimeric structure of VWF enables it to bind several ligands simultaneously and binding domains for integrins and platelet receptors have been identified on its subunits [15]. Direct interactions between VWF and tumor cells have been reported, involving $\alpha_{IIb}\beta_3$ [16], $\alpha_v\beta_3$ [17], or glycoprotein Ib [12]. In addition, it has been shown in a flow system that VWF was able to form a bridge between platelet integrin $\alpha_{IIb}\beta_3$ and an unidentified ligand on human colon carcinoma cell line LS174T [14]. Finally, *in vivo* experiments revealed that injection of rabbit serum against VWF in mice partially inhibits metastasis development induced by the different tumor cell lines [13].

Taken together, these different reports converge toward a potentially important role for VWF in metastasis development. However, most of these arguments remain indirect and we therefore decided to use VWF-deficient mice to directly determine VWF involvement in this process. We first studied the interaction of VWF with a murine transplantable tumor cell line, the melanoma B16-BL6 and we then developed an experimental metastasis model using the two different tumor cell lines.

Material and methods

Mice

The VWF-deficient mice [18] and wild-type mice used in this study were on a C57BL/6 background and were used between 6 and 10 weeks of age. Housing and experiments were carried out as recommended by the French regulations and Experimental Guidelines of the European Community.

Proteins

Purified plasma-derived human VWF was a gift from Dr Mazurier, LFB, Lille, France. For *in vitro* adhesion studies, the following recombinant human VWF were used: wild-type VWF (WT-VWF), VWF deleted of C1 and C2 domains (VWF-ΔC), VWF deleted of A1 domain (VWF-ΔA1), VWF deleted of A2 domain (VWF-ΔA2), and VWF mutated in the RGD sequence of the C1 domain (VWF-RGG). Construction, expression and purification of the different VWF variants have been described previously [19–24]. Purified proteins were dialyzed against 125 mM NaCl, 25 mM Hepes (pH 7.4), and stored at −80 °C. The cDNA encoding murine VWF was amplified by RT-PCR using total mouse lung RNA prepared from Balb/c mice (Sigma, Saint-Quentin-Fallavier, France). The cDNA was cloned into the pNUT-vector using *Spe*I (5′) and *Not*I (3′). The assembled cDNA contains an optimized Kozak sequence, but lacks 5′ or 3′ untranslated regions. The entire insert has been sequenced. The murine VWF construct was expressed in stably transfected baby hamster kidney cells, and purified from serum-free conditioned medium using the standard chromatographic methods.

Antibodies

A monoclonal antibody (Mab9) directed against the C1 domain of human VWF was used. This Mab inhibits interactions between VWF and $\alpha_{IIb}\beta_3$ and between VWF and $\alpha_v\beta_3$ [25,26].

For functional assays, we used monoclonal antibodies directed against different murine integrin subunits: a hamster anti-CD61 (clone 2C9.G2; Becton Dickinson, Le Pont-de-Claix, France), and a hamster anti-CD51 (clone H9.2B8; Becton Dickinson). Both these antibodies have been described as function-blocking antibodies, although the latter showed only low affinity [27]. We also used a rat anti-CD41 (clone MWReg30; Becton Dickinson). Control isotypes were used as negative controls. For flow cytometry analysis, the rat anti-CD41 (same clones as above) and the isotype control (rat IgG1) had been purchased directly coupled to fluorescein. For the anti-CD61 and anti-CD-51 antibodies, we used a mouse cocktail anti-Armenian and Syrian hamster IgG conjugated to phycoerythrin (Becton Dickinson).

Cell culture

The B16-BL6 murine melanoma cell line and the Lewis lung carcinoma (LLC) murine cell line were both cultured in Dulbecco's modified eagle medium (DMEM) (Sigma) containing 10% fetal calf serum (FCS) from Biowest (Abcys, Nuaillé, France), penicillin, streptomycin, and glutamine from Gibco (Invitrogen, Cergy-Pontoise, France), in 5% CO_2.

Cell adhesion assays

Microtiter plates (Greiner; MERCK Eurolab, Strasbourg, France) were coated overnight at 4 °C with human plasma or purified recombinant VWF (2 μg mL^{-1}), or with bovine serum albumin (BSA), heated 1 h at 70 °C (20 μg mL^{-1}). In one experiment, the wells were coated with either human or murine recombinant VWF at different concentrations. The wells were then rinsed in adhesion buffer (10 mM Hepes, 140 mM NaCl, 5.56 mM glucose, 5.4 mM KCl, 2 mM $CaCl_2$, 1 mM $MgCl_2$, 1 mM $MnCl_2$, pH 7.4). B16-BL6 cells were harvested with 0.5 mM EDTA, washed and resuspended in adhesion buffer containing 3% BSA, and 20 000 cells were added to the wells with or without various inhibitors. The cells were allowed to attach for 2 h at 37 °C. The cell suspension was then removed by aspiration and wells were rinsed twice with adhesion buffer. Cell adhesion was quantified by the measuring cellular phosphatase by addition of 130 μL para-nitro-phenol-phosphate (PNPP) (3 mg mL^{-1} in 50 mM acetate buffer, pH 5.5, 0.1% triton) as substrate. The reaction was stopped by addition of 70 μL 1 N NaOH and the reaction product was measured at 405 nm. Non-specific adhesion was

measured in wells coated with BSA. Given values are corrected for non-specific binding.

For inhibition assays, EDTA or Mab9 was added to the wells with the cell suspension at concentrations from 0.01 to 2.5 mM, or 0.1 to 1.5 μg mL^{-1}, respectively. Antibodies directed against integrin subunits (80 μg mL^{-1}) were preincubated with cells 30 min at room temperature.

Flow cytometry

B16-BL6 cells (10^6) in 100 μL of PBS-1% BSA were incubated with antibodies directed against α_v, α_{IIb} or β_3 or with the corresponding control isotypes (10 μg mL^{-1}) for 30 min at 4 °C. The cells were then washed twice with PBS–BSA, resuspended in 100 μL of the same buffer and if needed, further incubated with secondary antibodies coupled to phycoerythrin at 10 μg mL^{-1} for 15 min at 4 °C. After two additional washing steps, the cells were resuspended in 500 μL PBS–BSA. The samples were analyzed on a FACSCalibur flow cytometer (Becton Dickinson). Data for 10 000 events were collected and analyzed with the CELLQUEST software.

Subcutaneous injection of B16-BL6 or LLC cells

Wild-type and VWF-deficient mice were anesthetized and their back was shaved. A 30-gauge needle was used to inject 2.5×10^5 B16-BL6 or 5×10^5 LLC cells in 200 μL serum-free medium, subcutaneously into the dorsal skin of mice. The longest and the shortest diameters of tumors were measured daily with a digital caliper, during 12–14 days, then the mice were sacrificed. The volume of tumors was calculated using the formula $V = (LW^2)\pi/6$, where L and W are, respectively, the longest and the shortest diameters [28].

Experimental metastasis model

Subconfluent and low-passaged tumor cells were washed with PBS, detached by 0.5 mM EDTA, washed in serum-containing medium and then resuspended in cold serum-free medium. The cells were kept on ice until transplanted in mice. B16-BL6 cells (5×10^4 cells in 200 μL) or LLC cells (1.5×10^5 cells in 200 μL) were injected into the lateral tail vein. In one experiment, recombinant human VWF (10 μg) was added to the B16-BL6 cells just before injection in the VWF-deficient mice. After 14 days, the mice were euthanized, the lungs were removed and rinsed in 0.9% sodium chloride. The lungs were separated into individual lobes and the number of metastatic colonies on the surface was counted by an investigator unaware of mouse genotype.

Labeling of cells with (^{125}I)-iododeoxyuridine and quantitative analysis of the distribution of tumor cells after the introduction in the circulation

Melanoma B16-BL6 cells (10^6 cells) were plated on 100-mm dishes, and grown for 24 h in DMEM containing 10% FCS. Then, 1 μCi mL^{-1} 5-(^{125}I)-iodo-2′-deoxyuridine (ICN Pharmaceuticals France SA, Orsay, France) was added to the medium and the cells were incubated for an additional 24 h [29]. After one wash with PBS, the cells were detached as described above. (^{125}I)-iododeoxyuridine-labeled tumor cells were resuspended in cold serum-free medium, and 2×10^5 cells were injected into the lateral tail vein of mice. After 15 min, 1, 4, or 24 h, the mice were anesthetized by peritoneal injection of tribromoethanol (0.15 mL/10 g body weight) and 500 μL blood was collected by retro-orbital puncture into 10 μl 0.5 M EDTA. The mice were then euthanized and the lungs, liver and spleen were collected, rinsed in PBS, and placed in 70% ethanol. To eliminate free iodine liberated by dead tumor cells, the organs were washed extensively in 70% ethanol during 4 days. Residual radioactivity in blood and organs was measured with a gamma counter (1260 multigamma II; LKB, Wallace, Turku, Finland). In order to take into account radioactivity decay, two 200 μL aliquots of cell suspension were kept in parallel with the organs and blood samples and counted at the same time, thus allowing the determination of the injected dose. Data are presented as percent of the injected dose.

Histology analysis

Following the metastasis experiment, lungs were fixed in 10% buffered formalin and subsequently embedded in paraffin. Sections were stained with hematoxylin and eosin and evaluated for the presence of histological differences in the pulmonary tumor deposits between wild-type and VWF-deficient mice.

Data analysis and statistics

Data are presented as mean ± SD. Statistical analysis was performed using either the Student's unpaired *t*-test or the non-parametric Mann–Whitney *U*-test, as indicated in the figure legends, with the STATVIEW program (Statview version 5, SAS Institute Inc, Cary, NC, USA).

Results

In vitro *characterization of melanoma cells interaction with VWF*

We first tested whether B16-BL6 melanoma cells were able to adhere to VWF. B16-BL6 cell adhesion on VWF was time-dependent and increased until it reached a plateau after 1 h (data not shown). After 2 h, B16-BL6 cells were well spread and adhesion on VWF (Fig. 1A) was significantly higher than on BSA (Fig. 1B). The presence of manganese in the adhesion buffer was an absolute requirement for these cells to adhere to VWF. We next compared adhesion of B16-BL6 cells to recombinant human or murine VWF coated at different concentrations. Both types of VWF were similarly efficient in mediating tumor cell adhesion (Fig. 1C), suggesting that adhesion involves an evolutionary conserved region of the protein.

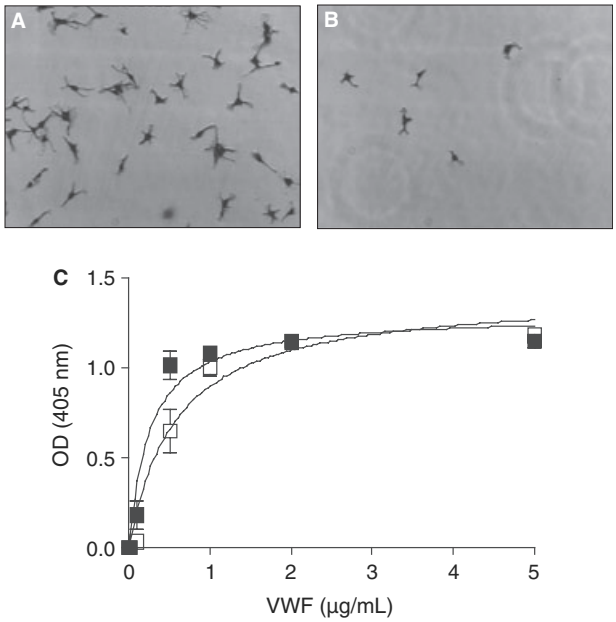

Fig. 1. B16-BL6 melanoma cell adhesion on VWF: B16-BL6 cells (2×10^4) were allowed to adhere for 2 h at 37 °C on microtiter plates coated with human plasma VWF (2 μg mL^{-1}) (A) or BSA (20 μg mL^{-1}) (B). Non-adherent cells were removed by washing wells with adhesion buffer and cells were photographed at an original magnification of ×100. (C) Recombinant human (closed squares) or murine VWF (open squares) coated at different concentrations was used as adhesion substrates for B16-BL6 cells. Non-adherent cells were removed by washing wells with adhesion buffer. Optical density at 405 nm is proportional to the phosphatase activity liberated by adherent cells.

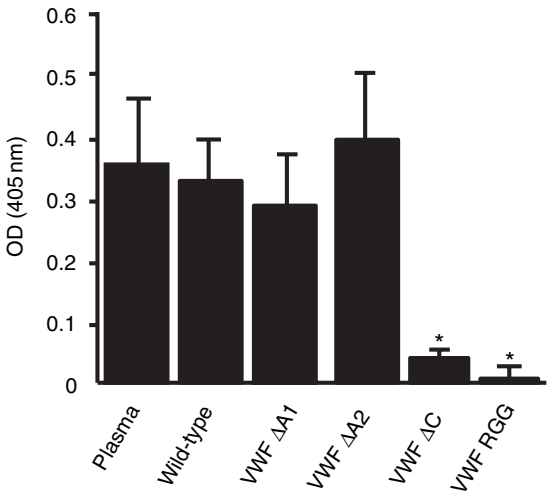

Fig. 2. B16-Bl6 melanoma cell adhesion on recombinant variants of VWF: B16-BL6 cells (2×10^4) were allowed to adhere for 2 h at 37 °C on microtiter plates coated with purified human plasma VWF or various purified recombinant human VWF (2 μg mL^{-1}): wild-type VWF (WT-VWF), VWF deleted of A1 domain (VWF-ΔA1), deleted of A2 domain (VWF-ΔA2), deleted of C1 and C2 domains (VWF-ΔC), and VWF mutated in the RGD sequence (VWF-RGG). Non-adherent cells were removed by washing wells with adhesion buffer. Optical density at 405 nm is proportional to the phosphatase activity liberated by adherent cells. $n = 3$ experiments; $^*P < 0.05$ (unpaired Student's *t*-test).

To identify this region, we performed adhesion assays using the recombinant human VWF, mutated or deleted of structural domains (Fig. 2). We first compared cell adhesion on human plasma VWF and on recombinant wild-type VWF. The results showed that B16-BL6 cells adhere similarly on both types of VWF, validating the use of recombinant VWF. Deletion of A1 or A2 domain had no significant effect on melanoma cell adhesion, suggesting that neither a glycoprotein Ib-like protein nor any VWF ligand binding to the A1 or A2 domains is involved in this interaction. In contrast, deletion of C domains (C1-C2) resulted in a significant decrease of B16-BL6 cell adhesion (> 75% inhibition, $P = 0.025$). To assess the potential implication of the RGD sequence present in the C1 domain of VWF, we used a recombinant VWF-RGG as adhesion substrate. The results showed a complete absence of B16-BL6 cell adhesion on VWF-RGG, suggesting the implication of an integrin as counter-receptor for VWF on the melanoma cells. To confirm this hypothesis, different inhibitors were used (Fig. 3A). Firstly, we performed adhesion assays in the presence of EDTA as calcium is necessary for integrin function. Increased doses of EDTA resulted in increased inhibition of B16-BL6 cell adhesion to VWF and a nearly complete inhibition with 2.5 mM EDTA (Fig. 3A). Next, we used Mab9, an antibody directed against human VWF that blocks its interaction with $\alpha_{IIb}\beta_3$ or $\alpha_v\beta_3$. A concentration of 1.5 μg mL^{-1} of Mab9 led to total inhibition of melanoma cell adhesion to VWF. We also performed adhesion

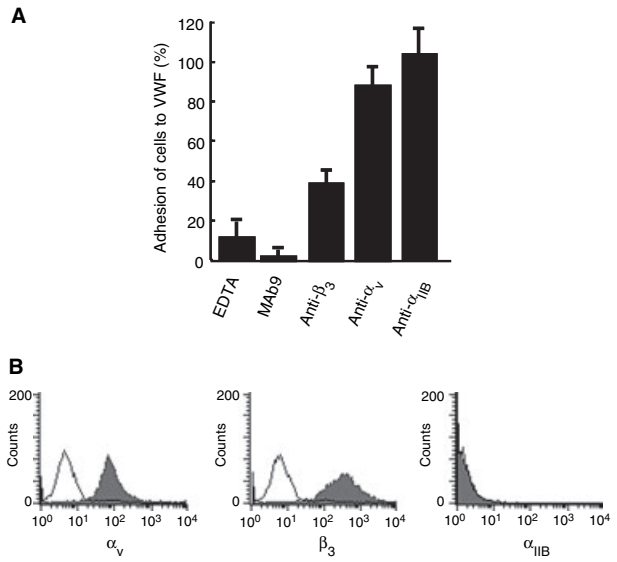

Fig. 3. B16-Bl6 melanoma cell adhesion on VWF in the presence of various inhibitors and expression of the various integrin receptors on these cells: (A) B16-BL6 cells (2×10^4) were allowed to adhere for 2 h at 37 °C on microtiter plates coated with human plasma VWF in the presence of EDTA (2.5 mM) or an Mab to VWF (Mab9) (1.5 μg mL^{-1}). Alternatively, cells were preincubated for 30 min at room temperature with antibodies to murine integrin subunits (β_3, α_v or α_{IIB}) (80 μg mL^{-1}) and were allowed to adhere to VWF for 30 min at 37 °C. Given values are represented as % of control adhesion measured without inhibitor and set at 100%. $n = 3$ experiments. (B) 10^6 B16-BL6 cells were stained for α_v, β_3,or α_{IIB} and analyzed by flow cytometry. White: isotype control. Grey: antibody directed against the indicated integrin subunit.

assays using antibodies directed against integrin subunits α_v, α_{IIb} and β_3. For this particular experiment, we shortened the adhesion time to 30 min to focus only on the early stage of adhesion. Using the anti-β3 antibody, we observed about 65% inhibition of cell adhesion to VWF. No significant inhibition of adhesion was observed using anti-α_v or α_{IIb} antibodies (Fig. 3A) but the anti-α_v was described as a very low affinity antibody [27], whereas the inhibitory activity of the anti-α_{IIb} is not clearly established [30]. In parallel, we tested the expression of these different integrin receptors on B16-BL6 cells by flow cytometry and found that there was a clear expression of both α_v and β_3 but no expression of α_{IIB} could be detected (Fig. 3B). Taken together, these observations strongly point to $\alpha_v\beta_3$ as the VWF receptor on the B16-BL6 tumor cells.

VWF is not implicated in tumor growth

To assess the role of VWF in tumor growth, B16-BL6 or LLC cells were injected subcutaneously in the dorsal skin of wild-type and VWF-deficient mice. The majority of mice from both genotypes developed a visible tumor within a few days: in each experiment one or two mice of each genotype did not develop any tumors during the whole duration of the experiment. Tumor size of wild-type and VWF-deficient mice increased regularly, and after 12 days, the tumor volume obtained with LLC cells reached 520.13 ± 144.91 mm^3 for the KO mice and 395.70 ± 90.95 mm^3 for the wild-type mice, ($P = 0.45$). For the B16-BL6 cells, the tumor volume measured after 14 days reached 866.7 ± 203.1 mm^3 for the KO mice and 575.3 ± 99.9 mm^3 for the wild-type mice ($P = 0.18$). These results demonstrate that despite a tendency for bigger tumors in the null-mice, VWF deficiency had no significant impact on tumor growth (Fig. 4).

Increased metastatic potential of tumor cells in VWF-deficient mice

The role of VWF in metastasis formation was tested in an experimental pulmonary metastasis model. Injection of B16-BL6 tumor cells in the tail vein of mice resulted in the development of dark metastatic colonies on the lungs.

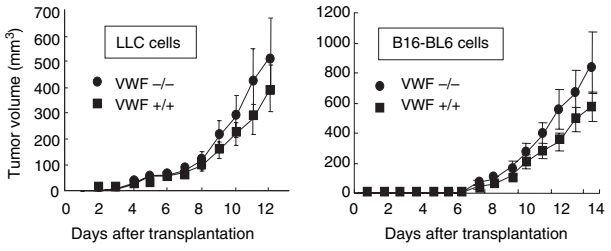

Fig. 4. Growth rate of subcutaneously transplanted LLC or B16-BL6 tumor cells: LLC (5×10^5) or B16-BL6 (2.5×10^5) cells were injected subcutaneously in the dorsal skin of wild-type (closed squares) ($n = 11$–13) and VWF-deficient (closed circles) ($n = 8$–9) mice. tumor volume was measured daily by calipation. Data represent mean ± SD. No significant difference was observed in tumor growth rate between the two genotypes.

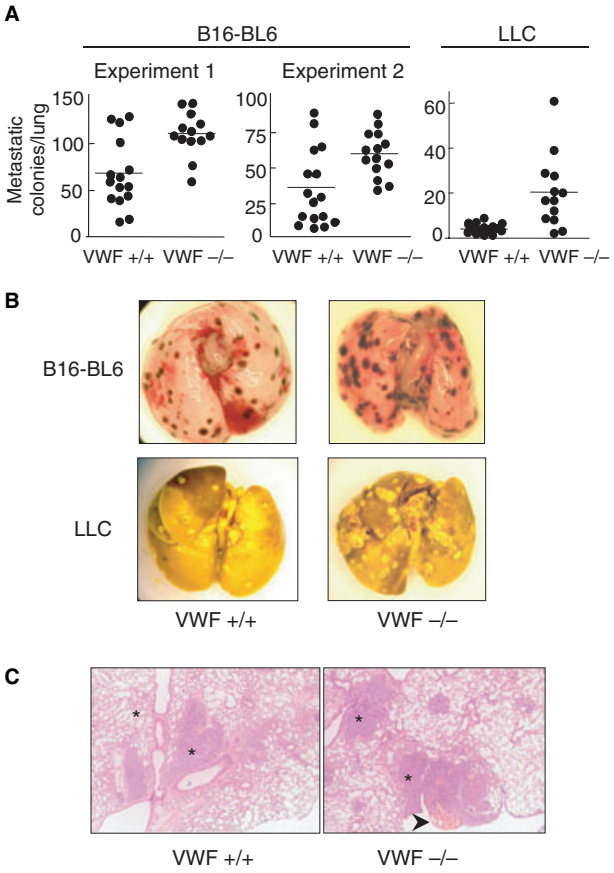

Fig. 5. Effect of VWF deficiency on experimental pulmonary metastasis formation: B16-BL6 melanoma cells (5×10^4) or LLC cells (1.5×10^5) were injected intravenously in wild-type (VWF+/+) and VWF-deficient (VWF−/−) mice by tail-vein injection. Lungs were isolated after 14 days and fixed. (A) Number of pulmonary nodules in VWF+/+ and VWF−/− mice in two independent experiments using B16-BL6 cells: Experiment 1: $n = 15$ for VWF+/+ and $n = 13$ for VWF−/−, $P = 0.0046$; Experiment 2: $n = 16$ for VWF+/+ and $n = 14$ for VWF−/−, $P = 0.041$. For the LLC experiment, $n = 15$ for VWF+/+ and $n = 13$ for VWF−/−, $P = 0.0006$ (Mann–Whitney, U2-tailed). With both cell types, the number of pulmonary nodules was significantly higher in VWF-deficient mice. (B) Representative examples of lungs with metastatic pulmonary foci of B16-BL6 melanoma cells and LLC cells in VWF+/+ and VWF−/− mice 14 days after cell injection. (C) Histological analysis of lung metastasis in VWF+/+ and VWF−/− mice after injection of B16-BL6 melanoma cells. After fixation, lungs were paraffin embedded, sectioned, and stained with hematoxylin/eosin. Both pleural and parenchymal (asterisks) metastases can be observed and the presence of local hemorrhage is visible in some tumor nodules (arrow). Although not visible on the picture, hemorrhage was also present in wild-type mice.

Similar observations were performed after injection of LLC cells with the notable difference that the metastatic colonies appeared white (Fig. 5B). Both wild-type and VWF-deficient mice developed pulmonary metastatic foci, showing that VWF is not absolutely required for hematogenous metastasis. However, for both cell types, VWF deficiency resulted in a significantly increased number of metastatic foci as shown in Fig. 5A,B. Two independent experiments performed with B16-BL6 cells are represented in Fig. 5A. Each point

represents the number of metastatic colonies counted on the lungs of one mouse. In the first experiment, an average of 67.7 ± 9.5 metastatic foci was counted in VWF+/+ mice (range 17–129), and 111.00 ± 6.6 in VWF−/− mice (range 77–144) ($P = 0.046$). In a second experiment, we counted an average of 34.5 ± 8 metastatic foci in VWF+/+ mice (range 5–86), and 57.7 ± 4.3 in VWF−/− mice (range 34–84) ($P = 0.041$). For LLC cells, we counted an average of 4.1 ± 0.6 foci in VWF+/+ mice (range 1–9), and 20.5 ± 4.5 in VWF−/− mice (range 2–61) ($P = 0.0006$).

These results suggest that the absence of VWF leads to an increased metastatic potential of the melanoma B16-BL6 and the LLC cells in mice. To compare the microscopic organization of the pulmonary foci between wild-type and VWF-deficient mice, we performed histological analysis of the lungs metastases after injection of B16-BL6 cells (Fig. 5C). No obvious qualitative difference was visible between the two genotypes. The presence of both parenchymal and pleural metastases was observed in lungs of wild-type and VWF-deficient mice. Some nodules had large necrotic areas associated with local hemorrhage in both genotypes.

In order to investigate whether restoring VWF plasma levels would rescue the observed phenotype, we co-injected B16-BL6 cells with human recombinant WT-VWF (10 μg) in VWF-deficient mice. After 2 weeks, we could not detect any statistical differences in the number of metastatic colonies in VWF-deficient mice injected with VWF compared with WT-mice ($P = 0.6$), whereas it was statistically different from VWF-deficient mice not injected with VWF ($P = 0.03$) (Table 1).

Early fate of tumor cells

To assess the early fate of circulating tumor cells in mice, B16-BL6 melanoma cells labeled with (^{125}I)-iododeoxyuridine were injected IV in wild-type and VWF-deficient mice. As the label from dead cells is rapidly excreted from the body, the residual radioactivity corresponds to live cells exclusively. This method revealed that within 15 min the majority of melanoma cells had disappeared from the circulation as only about 1% of B16-BL6 cells remains in blood of wild-type and VWF-deficient mice (data not shown). In contrast, about 70–85% of melanoma cells were found in the lungs within 15 min (Fig. 6), regardless of the mouse genotype. In the same time, radioactivity was around 3.5% in liver and 0.3% in spleen. The absence of VWF

Table 1 Number of metastatic colonies in VWF-deficient mice after restoration of VWF plasma level ($n = 4$–6)

	Pulmonary metastatic foci median (range)		
VWF+/+	141 (123–165)	$P = 0.6$	
VWF−/−	268 (108–407)		$P = 0.03$
VWF−/− injected with WT-VWF	134 (70–231)		

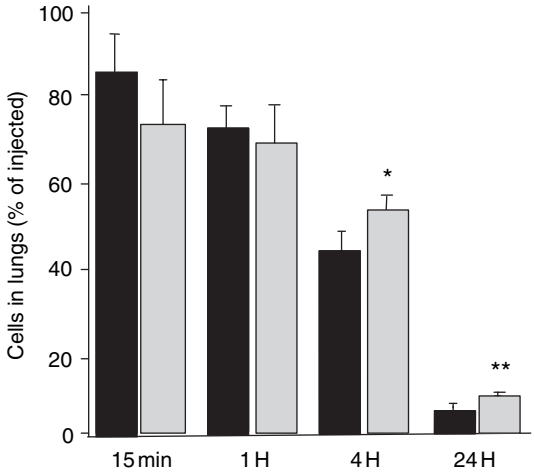

Fig. 6. Effect of VWF deficiency on the initial arrest and survival of ^{125}I-labeled B16-BL6 cells: B16-BL6 cells labeled with 5-(^{125}I) iodo-2′-deoxyuridine were injected in the lateral tail vein of wild-type (black bars) and VWF-deficient (grey bars) mice. The mice were euthanized at different time-points and the amount of radioisotope in the lungs was measured with a gamma counter. The data are presented as percent of injected dose (2×10^5 cells/49 000 cpm). $n = 4$–5 mice per time point. *$P = 0.13$. **$P = 0.0078$ (Unpaired Student's t-test).

did not influence the initial arrest of tumor cells in any of the organs tested. The number of viable melanoma cells in blood and organs decreased regularly in a time-dependent manner. Four hour after injection, there seemed to be a trend toward a larger number of tumor cells in the lungs of VWF-deficient mice compared with the wild-type mice, but this difference was not statistically significant (VWF−/−: 52.3% ± 3.4, VWF+/+: 43.0% ± 4.4, $P = 0.13$). However, after 24 h, it became clear that more B16-BL6 cells were present in the lungs of VWF-deficient mice compared with the wild-type mice (VWF−/−: 9.96% ± 0.59, VWF+/+: 6.10% ± 0.92, $P =$ 0,0078), suggesting that the absence of VWF favors the increased sustained adherence and/or survival of tumor cells *in vivo* (Fig. 6).

Discussion

Hematogenous tumor cell metastasis is a multifaceted process that depends on numerous cellular and molecular interactions within the vasculature. To metastasize successfully, circulating tumor cells must first arrest within the vasculature by adhering to blood vessel walls. So far, the mechanisms underlying this initial tumor cell–endothelial attachment have remained obscure. The present study originated from the possibility that VWF might participate in tumor cell–subendothelial interactions through a mechanism similar to that of platelet–subendothelial interactions in which VWF is a major player. As some tumor cells can form aggregates with platelets, VWF could mediate the adhesion of such heterotypic aggregates to the vascular endothelium *via* its direct association with the platelets and/or tumor cells. Interestingly, the data presented in this study, using VWF-deficient mice, suggest that although

VWF can indeed be considered as a determinant of the metastatic potential of the murine melanoma cell line B16-BL6, it appears to impede metastasis by reducing the sustained adherence and/or survival of tumor cells in lung vasculature.

The cell lines used in this study (B16-BL6 and LLC) were selected for different reasons: (i) they are both from a C57BL/6 genotype, similar to the VWF-deficient mice, (ii) they are highly metastatic, and (iii) fibrinogen deficiency as well as inhibitors of coagulation has previously been reported to inhibit their metastatic potential [28,31]. In order to test whether VWF could also interfere with this potential, we first decided to test its direct interaction with the B16-BL6 cell line. *In vitro* adhesion assays showed that B16-BL6 cells were able to adhere and spread on VWF and that murine or human VWF was similarly efficient in supporting that adhesion. The use of recombinant VWF (deleted of structural domains or mutated) allowed us to pinpoint the melanoma cell-binding site on VWF to the RGD sequence in the C1 domain. We next tried to identify the counter-receptor for VWF on the B16-BL6 cells. The calcium requirement, the identification of RGD as the binding site as well as the total inhibition of the interaction with Mab 9 to VWF suggested the involvement of an integrin receptor, most likely $\alpha_{IIb}\beta_3$ or $\alpha_v\beta_3$. The use of blocking antibodies confirmed the implication of a β_3-integrin but did not allow concluding as to which one was really interacting with VWF in this system because of the lack of good inhibitory antibodies. The absolute requirement for Mn^{2+} during adhesion assays indicates a major role for $\alpha_v\beta_3$, in accordance with the ability of Mn^{2+}-activated $\alpha_v\beta_3$ to support M21 human melanoma cell arrest when perfused over VWF [17]. These functional observations were supported by the fact that by FACs, we were able to detect α_v and β_3 subunits at the surface of B16-BL6 cells but no α_{IIB} could be found. Taken together, these different arguments support the idea that $\alpha_v\beta_3$ is the likely counter-receptor for VWF on B16-BL6 tumor cells.

Once we had established the capacity of VWF to interact with B16-BL6 cells, we used that same cell line in an experimental metastasis model using wild-type and VWF-deficient mice. We observed an increased number of pulmonary metastasis in the absence of VWF, a finding that was consistently repeated in the subsequent experiments. These unexpected results were confirmed with a second tumor cell line, the LLC cells, proving that they were not because of some specific and unique characteristics of the melanoma cell line. In contrast, tumor growth after subcutaneous inoculation of tumor cells, either LLC or melanoma, was not significantly affected by the absence of VWF.

Based on the ability of VWF to interact with tumor cells [14,16] as well as previous *in vivo* studies in mice [13], inhibition of VWF was expected to lead to an inhibition of metastasis formation. Indeed, using a polyclonal antibody to murine VWF, a 50% inhibition of tumor metastasis had been observed in wild-type mice injected with the different tumor cell lines [13]. Such apparent discrepancies between genetic ablations of genes and inhibition studies with pharmacological agents are not unheard of. For example, early work performed with antibodies suggested a pro-angiogenic role for α_v integrins while later results obtained in genetically altered mice did not support this hypothesis and even suggested an antiangiogenic role for these integrins [32]. Furthermore, *in vivo* experiments performed with antibodies, particularly polyclonal antibodies, can be very delicate to interpret. In the initial study with VWF, a number of antibodies of the polyclonal repertoire will still be able to bind to VWF without inhibiting its interaction with tumor cells. Such VWF–antibodies complexes, if bound to tumor cells, may facilitate the removal of these cells by the immune system, therefore leading to the observed metastasis inhibition.

The first step in understanding our metastasis results was to determine whether the observed phenotype was the direct or indirect consequence of the absence of VWF. Indeed, the absence of VWF is known to lead to the absence of Weibel–Palade bodies and to the mistargeting of the other proteins usually found in this compartment, among which P-selectin, tissue-type plasminogen activator, CD63, interleukin-8, endothelin [33], and recently the tie-2 ligand angiopoietin-2 [34]. As a result, the VWF-deficient mice can display unexpected phenotypes such as reduced inflammatory responses because of an impaired P-selectin expression [35]. Therefore, in order to test whether the absence of VWF was directly responsible for the increased metastasis, we studied metastasis formation in VWF-deficient mice injected simultaneously with B16-BL6 cells and VWF. Restoration of VWF plasma levels in these mice led to a correction of the phenotype and to a number of metastatic colonies similar to that found in wild-type mice, confirming the direct protective role of VWF in metastasis formation. Thus, it appears that the capacity of tumor cells to bind VWF, far from being an asset for their extravasation, could be detrimental and either lead to their clearance from the circulation or impair their sustained adherence in the lung tissues. To gain some insight in this mechanism, we have injected radiolabeled tumor cells in mice and followed their survival during the first 24 h. The following conclusions could be drawn from that experiment: (i) In both genotypes, 99% of the cells have left the circulation after 15 min suggesting that cellular extravasation is not a VWF-dependent step; (ii) At early time-points (15 min and 1 h), similar numbers of cells were present in the lungs or other organs of mice of both genotypes. These observations suggest that the initial arrest of tumor cells in the organs tested was not influenced by VWF, and that there was no premature clearance of tumor cells from the circulation; (iii) At later time-points (4 and 24 h), increased numbers of viable cells were found in the lungs of VWF-deficient mice. Indeed at 24 h, there was a 40% increase of live cells in the absence of VWF, similar to the 40% increase in B16-BL6 metastatic colonies in VWF-deficient mice after 2 weeks (Fig. 5A).

In conclusion, it appears that VWF can induce the death of tumor cells in the hours following their arrest in the lungs. Whether cell death is occurring because cells are prevented from consolidating their implantation in the lung tissues or through other mechanisms remains to be investigated.

Acknowledgements

This study was supported by grants from GEHT-ISTH (to VT), Marie Curie Research Training Network (#HPRN-CT-2002-00253 to RP), INSERM-NWO/ZonMW (#910-48-603 to CVD and PJL) and INSERM (Avenir research grant to CVD). We thank Erik Westein for expert technical assistance in cloning the murine VWF cDNA and Carina van Schooten for expert assistance in preparing the lung sections.

References

1 Trousseau A. Phlegmasia alba dolens. In: *Clinique Medicale de l'hotel Dieu de Paris 3*. Paris, France: JB Bailliere et Fils, 1865: 654–712.
2 Rickles FR, Falanga A. Molecular basis for the relationship between thrombosis and cancer. *Thromb Res* 2001; **102**: V215–24.
3 Loreto MF, De Martinis M, Corsi MP, Modesti M, Ginaldi L. Coagulation and cancer: implications for diagnosis and management. *Pathol Oncol Res* 2000; **6**: 301–12.
4 Browder T, Folkman J, Pirie-Shepherd S. The hemostatic system as a regulator of angiogenesis. *J Biol Chem* 2000; **275**: 1521–4.
5 Gasic GJ, Gasic TB, Stewart CC. Antimetastatic effects associated with platelet reduction. *Proc Natl Acad Sci USA* 1968; **61**: 46–52.
6 Nash GF, Turner LF, Scully MF, Kakkar AK. Platelets and cancer. *Lancet Oncol* 2002; **3**: 425–30.
7 Nieswandt B, Hafner M, Echtenacher B, Mannel DN. Lysis of tumor cells by natural killer cells in mice is impeded by platelets. *Cancer Res* 1999; **59**: 1295–300.
8 Dardik R, Kaufmann Y, Savion N, Rosenberg N, Shenkman B, Varon D. Platelets mediate tumor cell adhesion to the subendothelium under flow conditions: involvement of platelet GPIIb-IIIa and tumor cell alpha(v) integrins. *Int J Cancer* 1997; **70**: 201–7.
9 Felding-Habermann B, Habermann R, Saldivar E, Ruggeri ZM. Role of beta3 integrins in melanoma cell adhesion to activated platelets under flow. *J Biol Chem* 1996; **271**: 5892–900.
10 Borsig L, Wong R, Feramisco J, Nadeau DR, Varki NM, Varki A. Heparin and cancer revisited: mechanistic connections involving platelets, P-selectin, carcinoma mucins, and tumor metastasis. *Proc Natl Acad Sci USA* 2001; **98**: 3352–7.
11 Chen YQ, Trikha M, Gao X, Bazaz R, Porter AT, Timar J, Honn KV. Ectopic expression of platelet integrin alphaIIb beta3 in tumor cells from various species and histological origin. *Int J Cancer* 1997; **72**: 642–8.
12 Oleksowicz L, Dutcher JP, Deleon-Fernandez M, Paietta E, Etkind P. Human breast carcinoma cells synthesize a protein immunorelated to platelet glycoprotein-Ib alpha with different functional properties. *J Lab Clin Med* 1997; **129**: 337–46.
13 Karpatkin S, Pearlstein E, Ambrogio C, Coller BS. Role of adhesive proteins in platelet tumor interaction *in vitro* and metastasis formation *in vivo*. *J Clin Invest* 1988; **81**: 1012–9.
14 McCarty OJ, Mousa SA, Bray PF, Konstantopoulos K. Immobilized platelets support human colon carcinoma cell tethering, rolling, and firm adhesion under dynamic flow conditions. *Blood* 2000; **96**: 1789–97.
15 Sadler JE. Biochemistry and genetics of von Willebrand factor. *Annu Rev Biochem* 1998; **67**: 395–424.
16 Floyd CM, Irani K, Kind PD, Kessler CM. von Willebrand factor interacts with malignant hematopoietic cell lines: evidence for the presence of specific binding sites and modification of von Willebrand factor structure and function. *J Lab Clin Med* 1992; **119**: 467–76.
17 Pilch J, Habermann R, Felding-Habermann B. Unique ability of integrin alpha(v)beta 3 to support tumor cell arrest under dynamic flow conditions. *J Biol Chem* 2002; **277**: 21930–8.
18 Denis C, Methia N, Frenette PS, Rayburn H, Ullman-Cullere M, Hynes RO, Wagner DD. A mouse model of severe von Willebrand disease: defects in hemostasis and thrombosis. *Proc Natl Acad Sci USA* 1998; **95**: 9524–29.
19 Keuren JF, Baruch D, Legendre P, Denis CV, Lenting PJ, Girma JP, Lindhout T. von Willebrand factor C1C2 domain is involved in platelet adhesion to polymerized fibrin at high shear rate. *Blood* 2004; **103**: 1741–6.
20 Lankhof H, Damas C, Schiphorst ME, Ijsseldijk MJ, Bracke M, Sixma JJ, Vink T, de Groot PG. Functional studies on platelet adhesion with recombinant von Willebrand factor type 2B mutants R543Q and R543W under conditions of flow. *Blood* 1997; **89**: 2766–72.
21 Lankhof H, Wu YP, Vink T, Schiphorst ME, Zerwes HG, de Groot PG, Sixma JJ. Role of the glycoprotein Ib-binding A1 repeat and the RGD sequence in platelet adhesion to human recombinant von Willebrand factor. *Blood* 1995; **86**: 1035–42.
22 Sixma JJ, Schiphorst ME, Verweij CL, Pannekoek H. Effect of deletion of the A1 domain of von Willebrand factor on its binding to heparin, collagen and platelets in the presence of ristocetin. *Eur J Biochem* 1991; **196**: 369–75.
23 Lankhof H, van Hoeij M, Schiphorst ME, Bracke M, Wu YP, Ijsseldijk MJ, Vink T, de Groot PG, Sixma JJ. A3 domain is essential for interaction of von Willebrand factor with collagen type III. *Thromb Haemost* 1996; **75**: 950–8.
24 Lankhof H, Damas C, Schiphorst ME, Ijsseldijk MJ, Bracke M, Furlan M, de Groot PG, Sixma JJ, Vink T. Recombinant vWF type 2A mutants R834Q and R834W show a defect in mediating platelet adhesion to collagen, independent of enhanced sensitivity to a plasma protease. *Thromb Haemost* 1999; **81**: 976–83.
25 Denis C, Williams JA, Lu X, Meyer D, Baruch D. Willebrand factor contains a conformationally active RGD motif that mediates endothelial cell adhesion through the alpha v beta 3 receptor. *Blood* 1993; **82**: 3622–30.
26 Nokes TJ, Mahmoud NA, Savidge GF, Goodall AH, Meyer D, Edgington TS, Hardisty RM. Von Willebrand factor has more than one binding site for platelets. *Thromb Res* 1984; **34**: 361–6.
27 Schultz JF, Armant DR. Beta 1- and beta 3-class integrins mediate fibronectin binding activity at the surface of developing mouse peri-implantation blastocysts. Regulation by ligand-induced mobilization of stored receptor. *J Biol Chem* 1995; **270**: 11522–31.
28 Palumbo JS, Kombrinck KW, Drew AF, Grimes TS, Kiser JH, Degen JL, Bugge TH. Fibrinogen is an important determinant of the metastatic potential of circulating tumor cells. *Blood* 2000; **96**: 3302–9.
29 Fidler IJ. Metastasis: quantitative analysis of distribution and fate of tumor embolilabeled with 125 I-5-iodo-2′-deoxyuridine. *J Natl Cancer Inst* 1970; **45**: 773–82.
30 Nieswandt B, Echtenacher B, Wachs FP, Schroder J, Gessner JE, Schmidt RE, Grau GE, Mannel DN. Acute systemic reaction and lung alterations induced by an antiplatelet integrin gpIIb/IIIa antibody in mice. *Blood* 1999; **94**: 684–93.
31 Mueller BM, Reisfeld RA, Edgington TS, Ruf W. Expression of tissue factor by melanoma cells promotes efficient hematogenous metastasis. *Proc Natl Acad Sci USA* 1992; **89**: 11832–6.
32 Hynes RO. A reevaluation of integrins as regulators of angiogenesis. *Nat Med* 2002; **8**: 918–21.
33 de Wit TR, van Mourik JA. Biosynthesis, processing and secretion of von Willebrand factor: biological implications. *Best Pract Res Clin Haematol* 2001; **14**: 241–55.
34 Fiedler U, Scharpfenecker M, Koidl S, Hegen A, Grunow V, Schmidt JM, Kriz W, Thurston G, Augustin HG. The Tie-2 ligand angiopoietin-2 is stored in and rapidly released upon stimulation from endothelial cell Weibel-Palade bodies. *Blood* 2004; **103**: 4150–6.
35 Denis CV, Andre P, Saffaripour S, Wagner DD. Defect in regulated secretion of P-selectin affects leukocyte recruitment in von Willebrand factor-deficient mice. *Proc Natl Acad Sci USA* 2001; **98**: 4072–7.